Structural phase transition and molecular motions in $[(CH_3)_3CNH_3]_2[ZnCl_4]$ studied by ^1H NMR, differential scanning calorimetry, and x-ray diffraction

Keizo Horiuchi,* Shinsaku Uezato, Yumiko Yogi, Akihiko Abe, and Takanori Fukami
Faculty of Science, University of the Ryukyus, Nishihara-cho, Okinawa 903-0213, Japan

Ryo Takeishi
Department of Chemistry, University of Tsukuba, Tsukuba 305-8571, Japan

Ryuichi Ideda†
National Institute for Materials Science, Tsukuba 305-0003, Japan
(Received 29 April 2005; revised manuscript received 8 July 2005; published 18 November 2005)

The crystal structure of bis-*t*-butylammonium tetrachlorozincate $[(CH_3)_3CNH_3]_2[ZnCl_4]$ was determined at room temperature to be monoclinic with space group of $P2_1/n$ by the single-crystal x-ray diffraction method. Differential scanning calorimetry measurements show that the crystal undergoes a first-order structural phase transition at $T_{tr}=404$ K. An observed transition entropy of 26.3 J K^{-1} mol^{-1} suggests that this transition is of the order-disorder type. ^1H NMR measurements suggest that an isotropic reorientational motion of entire cations does not occur above T_{tr}. The phase transition is considered to arise from disordering of cations and anions among a number of sites.

DOI: 10.1103/PhysRevB.72.174114 PACS number(s): 64.70.Kb, 61.50.Ks, 61.10.−i, 65.40.Gr

I. INTRODUCTION

Bis-tetramethylammonium tetrahalometalates $[N(CH_3)_4]_2[MX_4]$ (M=Mn, Fe, Co, Cu, and Zn) belong to the A_2MX_4 family with the β-K_2SO_4 structure (space group *Pnma*), where MX_4^{2-} anion has a isolated tetrahedral structure. Many compounds in this family have already been extensively investigated[1] and a lot of works have been carried out especially on the chlorine compounds $[N(CH_3)_4]_2[MCl_4]$ because of their rich variety of phases (incommensurate, ferroelectric, ferroelastic, etc.) and successive phase transitions.[2]

The *t*-butylammonium ion $(CH_3)_3CNH_3^+$ is, in first approximation, nearly spherical similar to the tetramethylammonium ion $N(CH_3)_4^+$, and is an isoelectronic isomer to the tetramethylammonium ion.[3,4] Since the *t*-butylammonium ion, however, can make N-H···Cl hydrogen bonds in crystals, $[(CH_3)_3CNH_3]_2[MCl_4]$ is expected to show different properties compared with $[N(CH_3)_4]_2[MCl_4]$.

In the present investigation, we have determined the crystal structure of $[(CH_3)_3CNH_3]_2[ZnCl_4]$ at room temperature. Furthermore, the temperature dependences of the ^1H NMR spin-lattice relaxation time T_1 and the second moment M_2 of the resonance linewidth as well as the differential scanning calorimetry (DSC) were measured to study structural phase transitions and molecular motions in the title compound.

II. EXPERIMENTAL

The title compound was prepared by dissolving *t*-butylamine and $ZnCl_2$ in hydrochloric acid with the stoichiometric ratio, and then by slowly evaporating water from the solution in a desiccator over P_2O_5. The crystal obtained was recrystallized from water by a slow-evaporation method. The sample was identified by elemental analysis. Analytically Calculated: C, 27.02; H, 6.81; N, 7.88%. Found: C, 27.06; H, 6.71; N, 7.97%.

A single-crystal x-ray diffraction was measured on a Nonius CAD-4 diffractometer with the graphite-monochromated Mo $K\alpha$ radiation ($\lambda=0.71073$ Å) at room temperature. The intensity data were corrected for both Lorentz-polarization and absorption effects. The structure was solved by direct methods and refined by full-matrix least-squares methods. All of the calculations were performed on a VAX station 4000 with the MolEN program package.[5] Hydrogen atoms were not located and all non-hydrogen atoms were refined with anisotropic thermal parameters. Crystal data and experimental conditions are listed in Table I. An x-ray powder diffraction was measured using Cu $K\alpha$ radiation ($\lambda=1.54060$ Å) with a Philips X'Pert W3040/00 diffactometer at 300 and 420 K.

The ^1H NMR spin-lattice relaxation time T_1 was measured by a Brucker SXP-100 spectrometer at a Larmor frequency of 27.8 MHz (100–470 K) and by a home-made pulsed spectrometer[6] at frequency of 54.3 MHz (100–450 K). T_1 was determined by a 180°-τ-90° pulse sequence. The second moment M_2 of the resonance linewidth were measured with a Brucker SXP-100 spectrometer at a Larmor frequency of 40.0 MHz (110–460 K) using the solid-echo method[7] with a 90°_x-τ-90°_y pulse sequence.

A differential scanning calorimeter, DSC220, with a disk-station, SSC5200, from Seiko Instruments Incorporated was used for thermal measurements between about 130 K and the melting point. Samples of around 10 mg were employed and the heating and cooling rates were usually set at 10 and 5 K min^{-1}, respectively. The measurements were carried out under an atmosphere of dry N_2 gas with a flow rate of about 40 ml min^{-1} and repeated more than three times.

TABLE I. Crystal data, data collection, and structure refinement.

Crystal system	Monoclinic
Space group	$P2_1/n$
a/Å	17.382(2)
b/Å	12.221(1)
c/Å	17.646(2)
β/°	115.95(1)
Volume of unit cell/Å^3	3370.6(7)
Formula unit per cell	8
Density D_x/g cm^{-3}	1.401
D_m/g cm^{-3}	1.40(2)
Linear absorption coefficient/mm^{-1}	3.168
Crystal size/mm^3	$0.50\times0.44\times0.41$
Absorption correction type	Empirical via ψ scans
Transmission factor	0.7332–0.9990
Number of reflections measured	9119
Number of independent reflections	8456
Number of reflections used in refinement $I\geqslant3\sigma(I)$	3292
Maximum value of θ/deg.	28.41
R[a]	0.041
wR[a]	0.064
S	2.314
Number of parameters	272

[a]Refinement on F.

III. RESULTS AND DISCUSSION

A. Crystal structure

Results of the crystal structure analysis at room temperature are given in Tables I–III and Fig. 1. Average intensities $\langle I\rangle$ and standard deviations $\langle\sigma\rangle$ for some reflections are listed in Table IV, suggesting that the reflections with the following conditions are absent; $h+l=2n+1$ for $(h0l)$, $h=2n+1$ for $(h00)$, $k=2n+1$ for $(0k0)$, and $l=2n+1$ for $(00l)$. The results that a Laue group of $2/m$ was accepted and the systematic absences mentioned above were recognized indicate that a possible space group of $[(CH_3)_3CNH_3]_2[ZnCl_4]$ at room temperature is monoclinic $P2_1/n$, which is frequently observed in the A_2MX_4 family with the β-K_2SO_4 structure and is a subgroup of orthorhombic $Pnma$. The final R value was 0.041. There are two crystallographically inequivalent molecules, that is, two inequivalent $ZnCl_4^{2-}$ and four inequivalent t-butylammonium cations exist in a unit cell. Both of anions and cations are distorted tetrahedra, as can be seen from Fig. 1, where only nitrogen atoms in cations and zinc atoms in anions are labeled. In view of bond distances and angles in cations, we see that t-butylammonium ions $(CH_3)_3CH_3^+N1$ and $(CH_3)_3CH_3^+N4$ have a similar tetrahedron structure, and so do $(CH_3)_3CH_3^+N2$ and $(CH_3)_3CH_3^+N3$. t-butylammonium cations and $ZnCl_4^{2-}$ anions are linked together by an extensive network of N-H···Cl hydrogen bonds, listed in Table III with their N···Cl distances. N1 and N2 are involved in three N-H···Cl hydrogen bonds with relatively short N···Cl distances; on the other hand, N3 and N4 make four N-H···Cl hydrogen bonds. The hydrogen-bond network stabilizes the crystal packing. This crystal structure is isomorphous with bis t-butylammonium molybdate $[(CH_3)_3CNH_3]_2MoO_4$ which consists of two kinds of tetrahedral ions, i.e., a t-butylammonium cation and MoO_4^{2-} anion;[8] monoclinic, $P2_1/a$, $a=18.267(1)$, $b=13.738(1)$, $c=11.816(1)$ Å, $\beta=102.139(5)°$, $V=2899.2(2)$ Å^3, $Z=8$, $R=0.070$.

As shown below, this compound undergoes a structural phase transition at 404 K. The solid phases above and below 404 K are named as phase I and II, respectively. We could not determine the crystal structure of phase I, because single crystals are broken after experiencing the transition. Hence, we performed x-ray powder diffraction measurements at 300 and 420 K to obtain some informations on phase I, which results are displayed in Fig. 2. The data taken at 300 K was

TABLE II. Fractional atomic coordinates and equivalent isotropic displacement parameters (10^{-2} Å^2). U_{eq} is defined as one third of the trace of the orthogonalized U_{ij} tensor; $U_{eq}=\frac{1}{3}\Sigma_i\Sigma_j U_{ij}a_i^*a_j^*\mathbf{a}_i\cdot\mathbf{a}_j$.

Atom	x	y	z	U_{eq}
Zn1	0.11005(4)	0.24769(6)	0.45375(4)	4.13(1)
Cl11	0.0851(1)	0.0652(1)	0.4508(1)	6.23(4)
Cl12	0.2128(1)	0.2834(2)	0.4116(1)	7.07(4)
Cl13	−0.0083(1)	0.3447(2)	0.3738(1)	7.62(6)
Cl14	0.1484(1)	0.2921(1)	0.59081(9)	5.53(4)
Zn2	−0.07012(4)	−0.24377(6)	0.09355(4)	4.28(1)
Cl21	−0.0914(1)	−0.2548(1)	0.21112(9)	5.94(4)
Cl22	−0.0811(1)	−0.0691(1)	0.0470(1)	6.83(5)
Cl23	0.0693(1)	−0.2974(2)	0.1331(1)	5.64(4)
Cl24	−0.1599(1)	−0.3513(2)	−0.0103(1)	7.49(5)
N1	0.0123(3)	−0.3944(4)	0.3881(4)	6.21(2)
C11	0.1044(4)	−0.3520(5)	0.4282(4)	5.07(2)
C12	0.0974(5)	−0.2265(5)	0.4322(5)	7.22(2)
C13	0.1508(5)	−0.4016(7)	0.5158(4)	8.36(2)
C14	0.1458(4)	−0.3872(7)	0.3729(4)	7.85(2)
N2	0.3703(3)	0.1113(4)	0.5022(3)	5.70(1)
C21	0.4186(4)	0.1473(6)	0.5924(4)	5.70(2)
C22	0.4309(5)	0.2733(6)	0.5919(5)	8.49(2)
C23	0.3639(5)	0.1173(8)	0.6363(4)	8.11(2)
C24	0.5059(5)	0.0917(7)	0.6284(5)	8.74(2)
N3	0.1347(3)	−0.0515(5)	0.1312(3)	6.08(1)
C31	0.1716(4)	0.0003(6)	0.2174(3)	4.94(2)
C32	0.2613(6)	−0.0464(9)	0.2638(5)	11.40(3)
C33	0.1784(5)	0.1254(7)	0.2051(5)	9.37(3)
C34	0.1136(5)	−0.0210(9)	0.2589(5)	11.65(3)
N4	−0.0983(3)	−0.0560(4)	0.3457(3)	5.32(1)
C41	−0.1684(3)	0.0215(5)	0.2872(3)	4.18(1)
C42	−0.1347(4)	0.0698(6)	0.2278(4)	6.84(2)
C43	−0.2489(4)	−0.0494(7)	0.2383(4)	6.59(2)
C44	−0.1818(4)	0.1078(6)	0.3420(4)	7.35(2)

TABLE III. Bond distances (Å), bond angles (deg.), and N···Cl distances (Å).

Bond distance		Bond angle		N···Cl distances	
Zn1-Cl11	2.269(2)	Cl11-Zn1-Cl12	110.66(8)		
Zn1-Cl12	2.257(2)	Cl11-Zn1-Cl13	112.95(7)		
Zn1-Cl13	2.256(2)	Cl11-Zn1-Cl14	102.91(7)		
Zn1-Cl14	2.275(2)	Cl12-Zn1-Cl13	109.21(8)		
		Cl12-Zn1-Cl14	113.44(6)		
		Cl13-Zn1-Cl14	107.59(8)		
Zn2-Cl21	2.266(2)	Cl21-Zn2-Cl22	111.48(8)		
Zn2-Cl22	2.264(2)	Cl21-Zn2-Cl23	106.13(6)		
Zn2-Cl23	2.304(2)	Cl21-Zn2-Cl24	112.33(8)		
Zn2-Cl24	2.240(2)	Cl22-Zn2-Cl23	106.76(8)		
		Cl22-Zn2-Cl24	109.77(6)		
		Cl23-Zn2-Cl24	110.17(8)		
N1-C11	1.529(8)	N1-C11-C12	105.6(5)	N1···Cl13[a]	3.206(5)
C11-C12	1.542(9)	N1-C11-C13	108.5(6)	N1···Cl14[b]	3.228(6)
C11-C13	1.522(9)	N1-C11-C14	107.6(5)	N1···Cl2l	3.314(5)
C11-C14	1.51(1)	C12-C11-C13	111.5(6)		
		C12-C11-C14	112.5(7)		
		C13-C11-C14	110.7(6)		
N2-C21	1.504(7)	N2-C21-C22	107.3(5)	N2···Cl12	3.262(5)
C21-C22	1.55(1)	N2-C21-C23	106.6(5)	N2···Cl23[c]	3.200(6)
C21-C23	1.51(1)	N2-C21-C24	107.7(6)	N2···Cl24[d]	3.213(6)
C21-C24	1.52(1)	C22-C21-C23	111.3(7)		
		C22-C21-C24	109.3(6)		
		C23-C21-C24	114.4(4)		
N3-C31	1.508(7)	N3-C31-C32	105.6(6)	N3···Cl12[e]	3.663(7)
C31-C32	1.52(1)	N3-C31-C33	107.2(5)	N3···Cl22	3.383(6)
C31-C33	1.56(1)	N3-C31-C34	109.8(5)	N3···Cl22[f]	3.220(5)
C31-C34	1.51(1)	C32-C31-C33	108.7(6)	N3···Cl23	3.218(6)
		C32-C31-C34	114.9(6)		
		C33-C31-C34	110.2(7)		
N4-C41	1.532(7)	N4-C41-C42	105.7(5)	N4···Cl11	3.259(5)
C41-C42	1.53(1)	N4-C41-C43	106.7(5)	N4···Cl11[b]	3.499(6)
C41-C43	1.547(8)	N4-C41-C44	107.4(4)	N4···Cl14[b]	3.345(6)
C41-C44	1.52(1)	C42-C41-C43	111.1(5)	N4···Cl21	3.436(6)
		C42-C41-C44	112.4(6)		
		C43-C41-C44	113.0(6)		

[a] $x, y-1, z$.
[b] $\bar{x}, \bar{y}, \bar{z}+1$.
[c] $\bar{x}+\frac{1}{2}, y+\frac{1}{2}, \bar{z}+\frac{1}{2}$.
[d] $x+\frac{1}{2}, \bar{y}-\frac{1}{2}, z+\frac{1}{2}$.
[e] $\bar{x}+\frac{1}{2}, y-\frac{1}{2}, \bar{z}+\frac{1}{2}$.
[f] $\bar{x}, \bar{y}, \bar{z}$.

well analyzed by $a=17.38(2)$, $b=12.22(1)$, $c=17.65(2)$ Å, $\beta=115.95(10)°$. These values are in good agreement with those obtained by the single-crystal method listed in Table I. However, we could not analyze the data taken at 420 K. The powder pattern of phase I is as complicated as that of phase II, suggesting that the symmetry of phase I is not so higher than that of phase II.

B. DSC

A single heat anomaly due to a structural phase transition was observed at 404±2 K in the thermal measurements between about 130 K and the melting point of 502±2 K. The results are given in Table V and Fig. 3. Since a thermal hysteresis of 10±1 K was observed and a shape of observed DSC peak was sharp, the phase transition is a first order one.

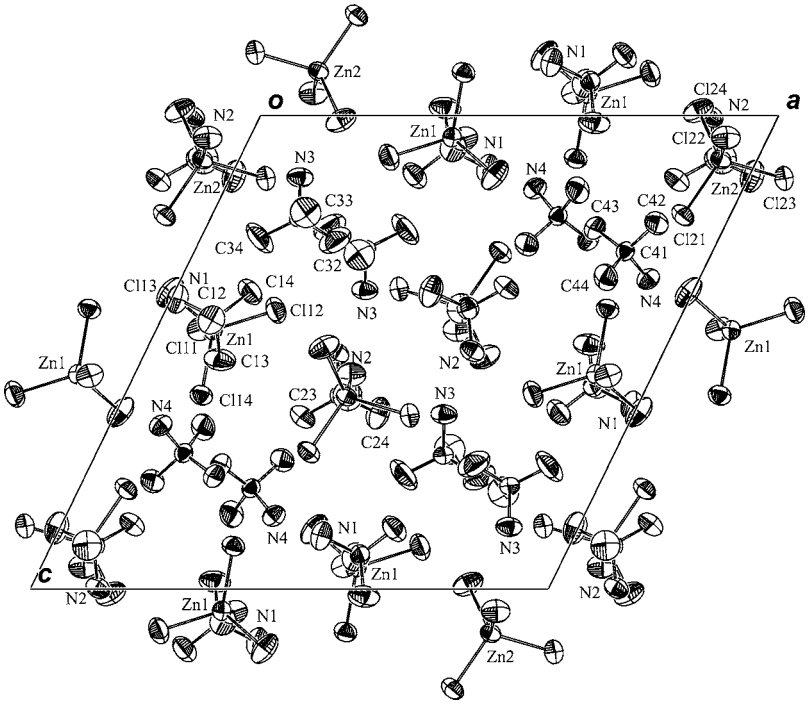

FIG. 1. Projection of the unit cell onto the *ac*-plane drawn using ORTEP with 50%-probability-displacement ellipsoids.

A transition enthalpy ΔH of 10.6 ± 0.1 kJ mol^{-1} and a transition entropy ΔS of 26.3 ± 0.3 J K^{-1} mol^{-1} were obtained. This large value of observed ΔS, comparable to an entropy change of 26.3 ± 0.3 J K^{-1} mol^{-1} observed at the fusion of 502 K, suggests that the phase transition is of the order-disorder type.

It is well known that a transition entropy larger than fusion entropy ΔS_f is observed for transitions to a liquid-crystal or plastic phase. Moreover, for the last two decades we have observed transitions with large entropy changes in *n*-alkylammonium chlorides $C_nH_{2n+1}NH_3Cl$ $(n=3-10,12)$ and some other ionic compounds having *n*-alkylammonium cations. For example, $(n\text{-}C_5H_{11}NH_3)_2ZnCl_4$, its $\Delta S_f=33$ J K^{-1} mol^{-1}, undergoes atructural phase transitions at 250 and 350 K with $\Delta S=14$ and 26 J K^{-1} mol^{-1}, respectively.[9] The total entropy change of 40 J K^{-1} mol^{-1} is larger than $\Delta S_f=33$ J K^{-1} mol^{-1}. The highest-temperature solid phase above 350 K is highly disordered, that is, alkylammonium chains perform uniaxial rotations about their molecular long axes whose orientations are also disordered and two-dimensional translational self-diffusions.[10] Hence, a large ΔS comparable to ΔS_f being observed suggests that phase I is highly disordered.

An entropy change ΔS in an order-disorder phase transition can be interpreted in terms of the Boltzmann principle

$$\Delta S = R \ln(N_I/N_{II}), \quad (1)$$

where N_{II} and N_I are the number of distinguishable orientations or positions of ions allowed in phase II and I, respectively. Since the present crystal-structure analysis at room temperature shows that cations and anions are ordered in phase II, $N_{II}=1$. If an order-disorder type of transition occurs in connection with the orientations and/or positions of anions, 26.3 J K^{-1} mol^{-1} $=R \ln N_I$ leading to $N_I \approx 24$. If an order-disorder type of transition occurs in connection with the orientations and/or positions of cations, 26.3 J K^{-1} mol^{-1} $=2R \ln N_I$ leading to $N_I \approx 5$. If an NH_3^+ group and two CH_3 groups perform hindered rotations about the bond axis between the central C and the other CH_3 group, the nitrogen atom gains four disordered sites. Hence, the ΔS values obtained may be explained by the disordering of nitrogen atoms. We will be able to find out whether the cations perform such a thermal motion by the NMR measurements.

TABLE IV. Numbers of reflections N_{ref}, average intensities $\langle I\rangle$ and standard deviations $\langle\sigma\rangle$ for some reflections.

Reflections	N_{ref}	$\langle I\rangle$	$\langle\sigma\rangle$	Reflections	N_{ref}	$\langle I\rangle$	$\langle\sigma\rangle$
$h00$ $(h=2n)$	10	9663	62	$h00$ $(h=2n+1)$	9	4	14
$0k0$ $(k=2n)$	8	6858	59	$0k0$ $(k=2n+1)$	7	2	13
$00l$ $(l=2n)$	20	7474	50	$00l$ $(l=2n+1)$	20	6	14
$h0l$ $(h+l=2n)$	395	2264	25	$h0l$ $(h+l=2n+1)$	393	5	13

C. Molecular motions

A temperature dependence of M_2 in the range 110–460 K is represented in Fig. 4. The M_2 value of 8.9 G^2 was ob-

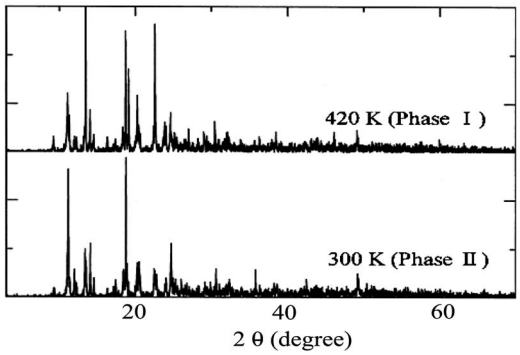

FIG. 2. X-ray powder diffraction patterns at 300 and 420 K.

TABLE V. Transition temperature T_c, order of transition, transition enthalpy ΔH, transition entropy ΔS, and thermal hysteresis ΔT_c.

T_c/K	Order	ΔH/kJ mol^{-1}	ΔS/J K^{-1} mol^{-1}	ΔT_c/K
404±2	1st	10.6±0.1	26.3±0.2	10±1
502±2	(fusion[a])	13.2±0.2	26.3±0.2	39±3

[a]Decomposed immediately after fusion.

served at 110 K and that was abruptly reduced to around 2 G^2 on heating. Between around 200 and 404 K, M_2 showed a constant value of 2.1±0.1 G^2. Just above the transition temperature, M_2 decreased slightly and took a constant value of 1.7±0.1 G^2 up to 460 K. In order to interpret the M_2 values obtained, we calculated M_2 values.[11] Since proton positions could not be located by the present crystal structure analysis, the calculation was carried out by assuming proton positions using standard values for a *t*-butylammonium ion. Moreover, we calculated M_2 values arising from only intracationic magnetic dipole-dipole interactions. The expected thermal motions are C_3 reorientations of the NH_3^+ group and three CH_3 groups about the C-N and the respective C-C bond axes, respectively, and C_3' reorientation of the *t*-butyl group $(CH_3)_3C$-about the C-N bond axis. Moreover, isotropic reorientation of entire cations that can average out the intracationic magnetic dipole-dipole interactions completely is expected. By taking some combinations of these motional modes, five motional states are considered. The calculated values are given in Table VI.

By comparing the observed and the calculated M_2 values, the cations are expected to undergo the C_3 reorientations of the NH_3^+ group and three CH_3 groups, even in 110 K. The almost constant value of 2.1±0.1 G^2 observed above 210 K in phase II suggests that the C_3' reorientation of the *t*-butyl group $(CH_3)_3C$-together with the C_3 reorientations of the CH_3 and the NH_3^+ groups are excited. However, some other motions must be excited in this temperature region, because the observed constant value of 2.1 G^2 in phase II and 1.7 G^2 in phase I are much smaller than 3.2 G^2 that can be larger if the interionic magnetic interactios are considered. Nevertheless, it is quite difficult to expect that an isotropic motion of entire cations occures in phase I, because the value of less than 1 G^2 is expected for that case.

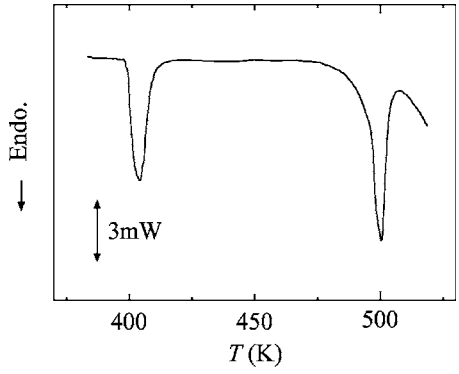

FIG. 3. A DSC curve of $[(CH_3)_3CNH_3]_2[ZnCl_4]$ recorded on heating.

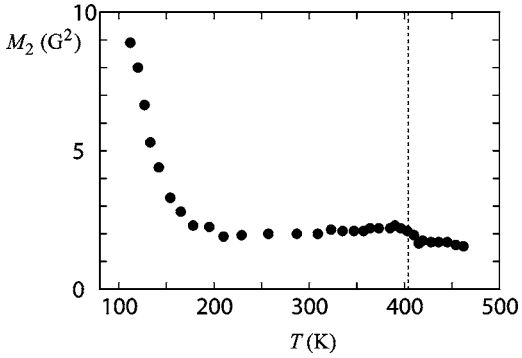

FIG. 4. A temperature dependence of M_2 of ^{1}H NMR absorptions. A vertical dotted line represents the phase transition temperature.

Temperature dependencies of ^{1}H NMR T_1 measured at 27.8 and 54.3 MHz are shown in Fig. 5. A discontinuity of T_1 was observed at the phase transition temperature. This also suggests that the transition is a first-order one. The observed T_1 curves gave a minimum around 200 K and a Larmor-frequency dependence was observed only on the low-temperature side of T_1 minimum. This temperature dependence is attributable to the magnetic dipolar relaxation caused by thermal molecular motions, and can be analyzed by the BPP equation,[12] expressed as

$$T_1^{-1} = C\left(\frac{\tau_c}{1+\omega_0^2\tau_c^2} + \frac{4\tau_c}{1+4\omega_0^2\tau_c^2}\right), \tag{2}$$

where C, ω_0, and τ_c are the motional constant, the angular Larmor frequency and the motional correlation time, respectively. Here τ_c is written by the following Arrhenius relationship:

$$\tau_c = \tau_0 \exp\left(\frac{E_a}{RT}\right), \tag{3}$$

where E_a is the motional activation energy.

The observed T_1 curves cannot be explained by the single BPP relation but are explainable by assuming that several motional modes are superimposed:

TABLE VI. Calculated second moments M_2 of ^{1}H NMR lines.

	M_2/G^2
Rigid	25.7
Reorientation of NH_3^+ group	19.7
Reorientation of three CH_3 groups	12.7
Reorientations of NH_3^+ group and three CH_3 groups	6.3
Reorientations of NH_3^+ group, three CH_3 groups and *t*-butyl group	3.2
Isotropic reorientation of entire cation	0

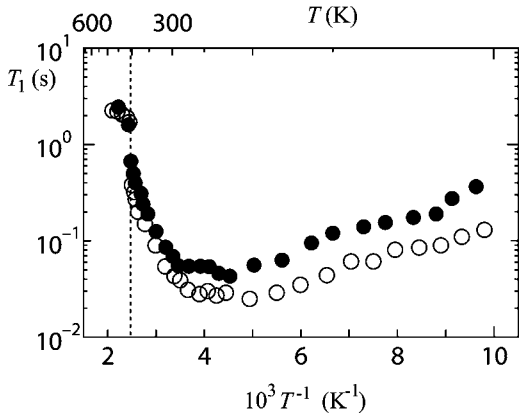

FIG. 5. Temperature dependencies of ^{1}H NMR T_1 measured at Larmor frequencies of 27.8 MHz (○) and 54.3 MHz (●). A vertical dotted line stands for the phase transition temperature.

$$T_{1,\mathrm{obs}}^{-1} = \sum_i T_{1i}^{-1}. \tag{4}$$

We analyzed the T_1 curves observed in phase II by superimposing six motional modes. The best fit T_1 curves obtained are displayed in Fig. 6 and the determined values of motional parameters and assigned motional modes are listed in Table VII. The assignment of motional modes was carried out by

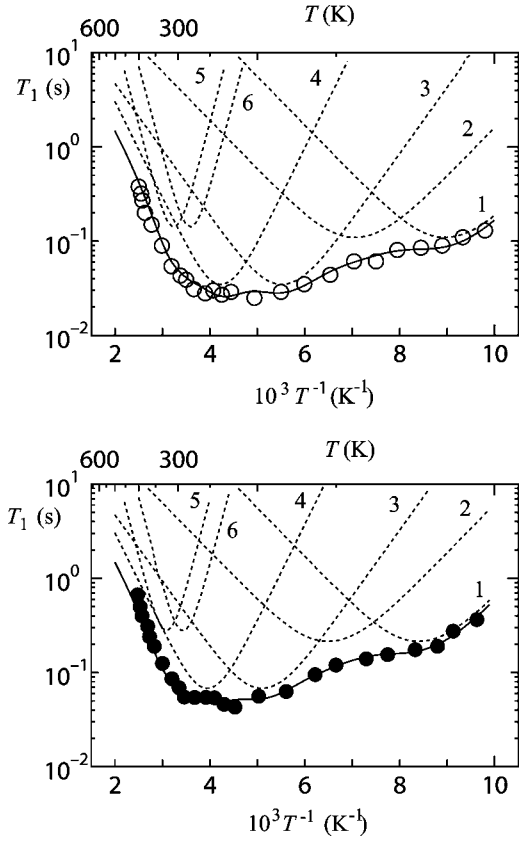

FIG. 6. The best-fitted calculated curves for ^{1}H NMR T_1 measured at 27.8 MHz (○) and 54.3 MHz (●). Broken curves and numbers indicate contributions from respective molecular motions (see Table VII).

TABLE VII. Motional parameters and motional modes of *t*-butylammnonium cations determined from ^{1}H NMR T_1 data. Numbers on the left-hand side correspond to those in Fig. 6.

	E_a/kJ mol^{-1}	$\tau_0/10^{-13}$ s	$C^a/10^9$ s^{-2}	Motional mode
1	9.88	8.0	1.1 (1.4)	NH_3^+ groups in cation 1
2	9.89	3.5	1.1 (1.4)	NH_3^+ groups in cation 2
3	13.4	4.7	3.5 (3.2)	CH_3 groups in cation 1
4	19.5	1.7	3.5 (3.2)	CH_3 groups in cation 2
5	36.8	2.1×10^{-2}	0.86 (0.74)	*t*-butyl groups in cation 1
6	35.8	6.8×10^{-3}	0.86 (0.74)	*t*-butyl groups in cation 2

[a]Values in parentheses are evaluated from Eq. (5) using the calculated second moments given in Table VI.

taking into account the discussion on M_2 given above. The motional parameter C in equation (2) is related to the M_2 reduction ΔM_2, due to the onset of the motion in question, as given by[13]

$$C = \frac{2}{3}\gamma^2 \Delta M_2, \tag{5}$$

where γ is the gyromagnetic ratio. The calculated vlues of C are listed in parenthesis in Table VII. We see that three motional modes, reorientations of the NH_3^+ group, three CH_3 groups and the *t*-butyl group $(CH_3)_3C$-, are responsible for the observed T_1 curves. Although four crystallographically inequivalent *t*-butylammonium cations exist in a unit cell, we found that we can group the four cations into two, each of them consists of two cations, from the point of view of molecular motions. It seems that the crystallographical data in this study also support this grouping. As mentioned in Sec. III A, four crystallographically inequivalent *t*-butylammonium cations can be divided into two groups according to bond distances and angles in cations or N···Cl hydrogen-bond scheme. Here these two cations are named as cation 1 and cation 2. The C_3' reorientation of the *t*-butyl groups are excited in the high-temperature region in phase II. The correlation times of the motion in cation 1 and cation 2 are 8.6×10^{-6} and 2.8×10^{-6} s, respectively, at 200 K, which satisfy the M_2 reduction observed below 200 K. Therefore, this T_1 analysis is consistent with the M_2 analysis given in the beginning of this section.

This analysis shows that the NH_3^+ motion did occur at the lowest temperature with the activation energies of 9.88 and 9.89 kJ mol^{-1}, which are smaller than those for the CH_3 groups (13.4 and 19.5 kJ mol^{-1}). This is surprising because a higher activation energy for NH_3^+ than for CH_3 is generally observed.[14] A higher activation energy for CH_3 than for NH_3^+ is reported for $[(CH_3)_3CNH_3]_2TeCl_6$,[15] and MO calculations on potential energies for the C_3 rotation of CH_3 and NH_3^+ groups in $(CH_3)_3CNH_3^+$ revealed that E_a values for the CH_3 and NH_3^+ groups are mostly due to the internal varrier to the rotations and the varrier height for the rotation of NH_3^+ is lower than for that of CH_3 owing to the C-N bond longer than the C-C bond.[14] In fact, comparable bond lengths of

C-C (1.51–1.57 Å) and C-N (1.542–1.548 Å) are observed in $[(CH_3)_3CNH_3]_2TeCl_6$,[16] which values contrast with normal C-C and C-N bond lengths of 1.54 and 1.47 Å, respectively. For the present complex, averaged C-C and C-N bond lengths are 1.53 and 1.52 Å, respectively.

Furthermore, we see that τ_0 values obtained for the C_3' reorientation of the *t*-butyl group are very small. Analyzing the T_1 data, the motional correlation time τ_c is expressed as Eq. (3). To be more exact, however, τ_c should be expressed as

$$\tau_c = \tau_0' \exp\left(\frac{\Delta G_a}{RT}\right), \tag{6}$$

where ΔG_a is the free energy of activation. In $\Delta G_a = \Delta H_a - T\Delta S_a$, $\Delta H_a \sim E_a$. Hence from Eqs. (3) and (6) we obtain

$$\tau_0 = \tau_0' \exp\left(-\frac{\Delta S_a}{R}\right). \tag{7}$$

This relation shows that an entropy effect results in the small values of τ_0. A site disordering of methyl groups are considered to bring about this effect. Since such a disorder can reduce M_2 values, this can be responsible for the fact that the M_2 values observed between around 200 and 400 K are smaller than the calculated one.

D. Phase transition

It is reported that all complexes of TMA_2MX_4 (TMA $=[N(CH_3)_4]$) having an ionic ratio $r_{TMA}/(r_M+r_X)$ higher than 0.695 present a modulated structure on lowering temperature.[17] $[N(CH_3)_4]_2[ZnCl_4]$ has the ionic ratio of 0.730 and undergoes successive structural phase transitions including incommensurate-commensurate ones below room temperature.[18] On the other hand, $[(CH_3)_3CNH_3]_2[ZnCl_4]$ shows only a single phase transition at 404 K in the range around 130 K to the melting point of 502 K, although the value of its ionic ratio is similar to that in $[N(CH_3)_4]_2[ZnCl_4]$. This lattice stabilitiy of the title compound seems to arise from N-H···Cl hydrogen bond net works. According to the Cochran's theory, the lattice instability that leads to structural phase transitions in ionic crystals occurs via a subtle cancellation of the short-range interaction by the long-range Coulombic interaction.[19] For simplicity, we regard the molecular ions as point charges for the Coulombic interaction. Since the long-range interaction is inversely proportional to the unit-cell volume *V*, for crystals with a large *V* it is difficult to undergo phase transitions. $[N(CH_3)_4]_2[ZnCl_4]$ takes a monoclinic phase with space group of $P2_1/c$ and $Z=4$ between 161 and 182 K, and its unit-cell volume is 1654.1 $Å^3$.[20] This value is comparable to a half of 3370.6 $Å^3$ ($Z=8$) in $[(CH_3)_3CNH_3]_2[ZnCl_4]$. Hence, the long-range forces in the two compounds are similar to each other in first approximation. On the other hand, for a small displacement of ions, the short-range force works more effectively in the crystals having interionic hydrogen bonds than in the nonhydrogen bonding system, because cations can exist closer to anions in the former system. Since NH_3^+ is fairly strong base, N···Cl hydrogen bonds work more effectively than C···Cl ones. Therefore, the lattice stability of the title compound is explained qualitatively in terms of their N-H···Cl hydrogen-bonding net works on the basis of Cochran's theory.

A structural phase transition observed at 404 K in $[(CH_3)_3CNH_3]_2[ZnCl_4]$ is of the first order and the order-disorder. A large transition entropy of 26.3 J K^{-1} mol^{-1} was observed, and no dynamic disorder of the nitrogen position in a $(CH_3)_3CNH_3^+$ ion was found in phase I by the NMR measurements. Hence this large ΔS value will be explained by the disordering of both anions and cations, because 26.3 J K^{-1} mol^{-1} is too large to be ascribed to the disorder of only anions or cations. Probably, the disorder of ions in phase I is similar to that observed for $[N(CH_3)_4]_2[ZnBr_4]$.[21] It crystallizes in the orthorhombic space group *Pnma* at room temperature (phase I).[22] At 287.6 K it undergoes a second-order phase transition to a ferroelastic phase (phase II) with monoclinic space group $P2_1/a$.[23,24] A transition entropy of 8–9 J K^{-1} mol^{-1} has been observed.[25] The constituent ions are reported to be in disorder in phase I.[21] Each ion is considered to take, with an equal probability, two configurations which are related each other by the mirror reflection. The distance between each corresponding two disordered sites is very close. The same disordering of cations and anions is observed also for $[N(CH_3)_4]_2[ZnCl_4]$ in a paraelectric phase with space group of *Pmcn*.[26]

Since the tetrahedral cations and anions in $[(CH_3)_3CNH_3]_2[ZnCl_4]$, $[N(CH_3)_4]_2[ZnCl_4]$, and $[N(CH_3)_4]_2[ZnBr_4]$ can be, in the first approximation, assumed to be spherical but have a space for the disorder, they can easily go into a rotationally disordered state. However, the title compound has N-H···Cl hydrogen bond net works, which prevent the constituent ions from taking large displacements. A small M_2 decrease observed at the phase transition of 404 K seems to be explained by thermal motions of the ions jumping among some disordered sites that locate closely to each other. Judging from the observed ΔS value, the number of disordered sites and distances among disordered sites in $[(CH_3)_3CNH_3]_2[ZnCl_4]$ are larger than those in $[N(CH_3)_4]_2[ZnBr_4]$ and $[N(CH_3)_4]_2[ZnCl_4]$. In the previous section, we have pointed out that the methyl groups are disordered among several sites in phase II. In case of an order-disorder phase transition of second order, an ordered phase is not completely ordered and is considerably disordered near the phase transition temperature. This situation is described by the temperature variation of the potential well for the disordered sites; that is, in the ordered phase, the potential well is asymmetric and temperature-dependent, while in the disordered phase, a symmetric and temperature-independent potential well is formed. In this case, thermal jump motions among the asymmetric potential well affect NMR T_1 and M_2 even in the ordered phase. Although the observed phase transition in the present case is of the first order, thermal motions among the asymmetric well seem to be excited near the phase transition temperature of 404 K.

IV. CONCLUSION

$[(CH_3)_3CNH_3]_2[ZnCl_4]$ crystallizes in monoclinic with space group of $P2_1/n$ at room temperature. It undergoes a first-order structural phase transition at 404 ± 2 K with an entropy change of 26.3 ± 0.3 J K^{-1} mol^{-1}, which is driven by disordering of both cations and anions. No isotropically reorientational motion of entire cations occurs above 404 K. A number of distinguishable disordered sites are expected to be allowed above 404 K, and distances among disordered sites are relatively close.

ACKNOWLEDGMENTS

This work was partly supported by a Grant-in-Aid for Scientific Research No. 06640450 from the Ministry of Education, Science, Sports and Culture, Japan.

*Electronic address: horiuchi@sci.u-ryukyu.ac.jp
†Department of Chemistry, University of Tsukuba, Tsukuba 305-8571, Japan.

[1] *Incommensurate Phases and Dielectrics*, edited by R. Blinc and A. P. Levanyuk (North-Holland, Amsterdam, 1986).
[2] For example, H. Shimizu, N. Abe, N. Kokubo, S. Fujimoto, T. Yamaguchi, and S. Sawada, Solid State Commun. **34**, 363 (1980); K. Gesi, Ferroelectrics **66**, 269 (1986).
[3] M. Shabazi, S.-Q. Dou and Al. Weiss, Z. Naturforsch., A: Phys. Sci. **47**, 171 (1992).
[4] K. Horiuchi, Phys. Status Solidi A **201**, 723 (2004).
[5] C. K. Fair, *MolEN. An Interactive Intelligent System for Crystal Structure Analysis* (Enraf-Nonius, Delft, 1990).
[6] T. Kobayashi, H. Ohki, and R. Ikeda, Mol. Cryst. Liq. Cryst. Sci. Technol., Sect. A **257**, 279 (1994).
[7] J. G. Powles and J. H. Strange, Proc. Phys. Soc. London **82**, 6 (1963).
[8] P. Roman, A. S. Jose, A. Luque, J. M. Gutierrez-Zorrilla, and M. Martinez-Ripoll, Acta Crystallogr., Sect. C: Cryst. Struct. Commun. **50**, 1189 (1994).
[9] Y. Sakiyama, K. Horiuchi, and R. Ikeda, J. Phys.: Condens. Matter **8**, 5345 (1996).
[10] K. Horiuchi, H. Takayama, S. Ishimaru, and R. Ikeda, Bull. Chem. Soc. Jpn. **73**, 307 (2000).
[11] J. H. Van Vleck, Phys. Rev. **74**, 1168 (1948).
[12] N. Bloembergen, E. M. Purcell, and R. V. Pound, Phys. Rev. **73**, 679 (1948).
[13] G. Soda and H. Chihara, J. Phys. Soc. Jpn. **36**, 954 (1974).
[14] H. Ishida, Y. Kubozono, S. Kashino, and R. Ikeda, Z. Naturforsch., A: Phys. Sci. **47**, 1255 (1992).
[15] H. Ishida, S. Inada, N. Hayama, D. Nakamura, and R. Ikeda, Ber. Bunsenges. Phys. Chem. **95**, 866 (1991).
[16] H. Ishida and S. Kashino, Acta Crystallogr., Sect. C: Cryst. Struct. Commun. **48**, 1673 (1992).
[17] M. Amami and A. Ben Salah, J. Phys. Soc. Jpn. **73**, 1781 (2004).
[18] S. Sawada, T. Yamaguchi, H. Suzuki, and H. Shimizu, J. Phys. Soc. Jpn. **54**, 3129 (1985).
[19] W. Cochran, Adv. Phys. **9**, 387 (1960).
[20] H. Kasano, N. Koshiji, and H. Mashiyama, J. Phys. Soc. Jpn. **61**, 348 (1992).
[21] T. Asahi, K. Hasebe, and K. Gesi, J. Phys. Soc. Jpn. **57**, 4219 (1988).
[22] P. Trouelan, J. Lefebvre, and P. Derollez, Acta Crystallogr., Sect. C: Cryst. Struct. Commun. **40**, 386 (1984).
[23] K. Gesi, J. Phys. Soc. Jpn. **51**, 203 (1982).
[24] P. Trouelan, J. Lefebvre, and P. Derollez, Acta Crystallogr., Sect. C: Cryst. Struct. Commun. **41**, 846 (1984).
[25] R. Perret, Y. Beaucamps, G. Godefroy, P. Muralt, M. Ehrensperger, H. Arend, and D. Altermatt, J. Phys. Soc. Jpn. **52**, 2523 (1983).
[26] K. Hasebe, H. Mashiyama, N. Koshiji, and S. Tanisaki, J. Phys. Soc. Jpn. **56**, 3543 (1987).